

Ponderomotive-force potential and density scale length in a laser-driven plasma

Shen Wenda

Department of Physics, Shanghai University of Science and Technology, Shanghai, China

Zhu Shitong

*Center of Theoretical Physics, Chinese Center of Advanced Science and Technology (World Laboratory), Beijing, China
and Shanghai Institute of Optics and Fine Mechanics, Academia Sinica, Shanghai, China*

(Received 3 March 1986; revised manuscript received 21 September 1987)

The modification of the density profile caused by the ponderomotive force in a laser plasma is further studied. A completely self-consistent three-parameter family of solutions for the ponderomotive-force potential and density scale length in a steady-state laser plasma is first derived. The boundary and junction conditions are given by the self-similar solution. The obtained results are more accurate and rigorous than the previous results.

I. INTRODUCTION

The electric field structure and density profile in a laser plasma are one of the important research subjects for laser fusion. As is well known, the absorption and scattering of the laser and other physical processes in laser-irradiated targets are closely related to the specific form of the laser-induced density profile, which must be quantitatively studied to acquire a deeper understanding of the laser-plasma interaction.

The modification of the density profile and four possible types of density-profile structures caused by the ponderomotive force have been extensively investigated.¹ In particular, a plateau-like density profile has been analyzed in many works. Lee *et al.* first established self-consistent relations between N_2 , V_2 , N_1 , V_1 , and $|A_s|^2$ and the relation between A_0^2 and $|A_s|^2$, but the latter is derived with the approximation that the density in the underdense region equals the average of the upper and lower shelf densities.² They have not found the characteristic parameter L_c at the critical density surface which is of significance in the laser-plasma interaction. Estabrook *et al.* further derived a scaling law for the local scale length at the critical density surface on the assumption that the density profile between the critical and sonic points is locally linear.³ In their treatment, the solution in the form of an Airy function is extended to the vacuum boundary so as to join the field at the sonic point to the incident laser field. Such a procedure is feasible for lower-intensity incident light. In this case the density profile is still gentle near the critical density region, and its density scale length is close to that in the underdense region. Under higher-intensity incident light, the density gradient near the critical density region obviously steepens, and the modified density should be approximately replaced by a doubly linear distribution with different density scale lengths. Then the above procedure is no longer useful for higher-intensity incident light. As Estabrook *et al.* have mentioned, their results are only valid for $0.1 < v_{os}/v_e < 1$. Besides, the conclusion in Refs. 2 and 3 that the oscillation in the underdense region is

characterized by equal amplitude and equal wavelength is unrealistic.

Recently, Xu *et al.* have tried to improve these results without using the above assumption for the linear critical density profile.⁴ However, their analysis is only valid for real field because $|dA/dx| \neq |A|/dx$ for a complex field. For a real-field amplitude A_0 , the stationary-wave field function

$$A(\xi) = 2A_0 \sin \left[-kL \left(2\sqrt{\epsilon} + \ln \frac{1-\sqrt{\epsilon}}{1+\sqrt{\epsilon}} + C \right) \right] / \epsilon^{1/4}$$

in the underdense region given in Ref. 4 cannot be practically matched with a plane electromagnetic wave in a vacuum. In other words, A_0 is not the true real-field amplitude in a vacuum because

$$\sin \left[-kL \left(2\sqrt{\epsilon} + \ln \frac{1-\sqrt{\epsilon}}{1+\sqrt{\epsilon}} + C \right) \right] \neq \frac{1}{2}.$$

Moreover, in the underdense region $d|A|^2/d\xi$ does not vanish everywhere, and it is unreasonable to assume that the density in this region is not modified by the ponderomotive force. Therefore their treatment is not completely self-consistent. In this paper we will give the exact analytical derivation of the density scale length for a complex field and establish the connection between A_0^2 and $|A_s|^2$ on the basis of the steady-state model.

II. FUNDAMENTAL EQUATIONS AND SELF-CONSISTENT GENERAL SOLUTION

When an *s*-polarized plane electromagnetic wave $\mathbf{E} = E_0 \exp(-i\omega t + ikx \cos\theta +iky \sin\theta) \mathbf{e}_z$ obliquely impinges onto an isothermal plasma which is freely expanding along the *x* direction, a one-dimensional isothermal plasma flow is developed under the action of the ponderomotive force, and its behavior is governed by the hydrodynamic equations for ions and the wave equations for the electric field \mathbf{E} ,

$$\frac{\partial n}{\partial t} + \frac{\partial(nv)}{\partial x} = 0, \quad (1)$$

$$\frac{\partial v}{\partial t} + v \frac{\partial v}{\partial x} + C_s^2 \frac{\partial \ln n}{\partial x} = - \frac{Ze^2 \partial |\mathbf{E}|^2}{4Mm\omega^2 \partial x}, \quad (2)$$

$$\nabla^2 \mathbf{E} - \frac{\partial^2 \epsilon \mathbf{E}}{c^2 \partial t^2} = 0, \quad (3)$$

where $C_s = (ZT_e/M)^{1/2}$ is the sound speed, $\epsilon = 1 - 4\pi e^2 n / m\omega^2$ is the dielectric constant of the plasma, v is the flow velocity, m (M) is the electron (ion) mass, Z is the charge state, n is the plasma density, e and T_e are the electron charge and temperature, and ω and k are the frequency and wave number of the incident light. Here we have taken no account of the effects of the ionization dynamics in the corona, the ablation dynamics in the target interior, and the electron-electron and electron-ion collisions for simplicity.

Inspection of Eqs. (1)–(3) shows that these equations have a steady-state solution. We are now in a position to derive an exact self-consistent solution for a complex field. In the frame of reference moving with the density jump, Eqs. (1)–(3) can be rewritten as

$$\frac{\partial(VN)}{\partial \xi} = 0 \quad \text{or} \quad VN = N_s, \quad (4)$$

$$V \frac{\partial V}{\partial \xi} + \frac{1}{N} \frac{\partial N}{\partial \xi} = - \frac{1}{4} \frac{\partial |A|^2}{\partial \xi}, \quad (5)$$

$$\frac{\partial^2 A}{\partial \xi^2} + (1-N)A = 0, \quad (6)$$

where $V = v/C_s$, $N = n/n_c \cos^2 \theta$, $A = eE/m\omega v_e$, $\xi = kx \cos \theta$, $v_e = (T_e/m)^{1/2}$ is the electron thermal speed, and $\frac{1}{4} |A|^2$ is the ponderomotive-force potential.

Substituting Eq. (4) into Eq. (5) yields

$$\left[V - \frac{1}{V} \right] \frac{\partial V}{\partial \xi} = - \frac{1}{4} \frac{\partial |A|^2}{\partial \xi}. \quad (7)$$

Multiplying Eq. (6) and its conjugate equation by A^* and A , respectively, and adding the obtained equations, we get

$$\frac{\partial^2 |A|^2}{\partial \xi^2} - 2 \left| \frac{\partial A}{\partial \xi} \right|^2 + 2(1-N) |A|^2 = 0. \quad (8)$$

Multiplying Eq. (6) and its conjugate equation by $\partial A^*/\partial \xi$ and $\partial A/\partial \xi$, respectively, and adding the obtained equations, we get

$$\frac{\partial}{\partial \xi} \left| \frac{\partial A}{\partial \xi} \right|^2 + (1-N) \frac{\partial |A|^2}{\partial \xi} = 0. \quad (9)$$

Integrating Eq. (7) and using the condition of the sonic point that $V=1$, $N=N_s$, $|A|=|A|_s$, and $|\partial A/\partial \xi|=|\partial A/\partial \xi|_s$, we obtain

$$|A|^2 = |A_s|^2 - 2(V^2 - 2 \ln V - 1), \quad (10)$$

$$|A|^2 = |A_s|^2 - 2(N_s^2/N^2 - 2 \ln N_s + 2 \ln N - 1). \quad (11)$$

Integrating Eq. (9) yields

$$\begin{aligned} \left| \frac{\partial A}{\partial \xi} \right|^2 &= 2(V^2 - 2 \ln V - 1) - 4N_s \left[V + \frac{1}{V} - 2 \right] \\ &+ \left| \frac{\partial A}{\partial \xi} \right|_s^2. \end{aligned} \quad (12)$$

Inserting Eqs. (7), (10), and (12) into Eq. (8), we obtain the differential equations for the velocity,

$$\frac{\partial^2 V}{\partial \xi^2} + \frac{1}{2} P(V) \left[\frac{\partial V}{\partial \xi} \right]^2 = \frac{1}{2} Q(V) \quad (V \neq 1), \quad (13)$$

$$\left[\frac{\partial V}{\partial \xi} \right]^2 = \frac{1}{4} (1-N_s) |A|_s^2 - \frac{1}{4} \left| \frac{\partial A}{\partial \xi} \right|_s^2 \quad (V=1), \quad (14)$$

with

$$P(V) = 2(1 + 1/V^2)(V - 1/V)^{-1}, \quad (15)$$

$$\begin{aligned} Q(V) &= \left\{ (1 - N_s/V) [|A_s|^2 - 2(V^2 - 2 \ln V - 1)] \right. \\ &\quad - 2(V^2 - 2 \ln V - 1) + 4N_s(V + 1/V - 2) \\ &\quad \left. - \left| \frac{\partial A}{\partial \xi} \right|_s^2 \right\} (V - 1/V)^{-1}. \end{aligned} \quad (16)$$

Let $\partial V/\partial \xi \equiv Y^{1/2}$, then Eq. (13) becomes

$$\frac{dY}{dV} + P(V)Y = Q(V). \quad (17)$$

The solution of Eq. (17) is

$$\begin{aligned} Y &= \left[\frac{\partial V}{\partial \xi} \right]^2 = \exp \left[- \int P dV \right] \left[\int Q(V) \exp \left[\int P dV \right] dV + C \right] \\ &= \left[\frac{V}{V^2 - 1} \right]^2 \left[\left[|A_s|^2 + 4 - 8N_s - \left| \frac{\partial A}{\partial \xi} \right|_s^2 \right] (V^2/2 - \ln V) - V^4 - 4(\ln V)^2 + 4V^2 \ln V \right. \\ &\quad \left. - N_s(V + 1/V)(|A_s|^2 + 4 \ln V) + 2N_s V^3 - 2N_s/V + C \right], \end{aligned} \quad (18)$$

where C is the constant of integration. The requirement that the above equation should be identical with Eq. (14) as $V \rightarrow 1$ gives

$$C = \frac{1}{2} \left| \frac{\partial A}{\partial \xi} \right|_s^2 - \frac{1}{2} |A_s|^2 - 1 + 4N_s + 2N_s |A_s|^2.$$

Then Eq. (18) can be rewritten in the form

$$Y^{1/2} = \frac{\partial V}{\partial \xi} = \pm \left| \frac{V}{V^2 - 1} \right| \left[\left(\left| \frac{A_s}{2} \right|^2 - (V^2 - 2 \ln V - 1) - \frac{1}{2} \left| \frac{\partial A}{\partial \xi} \right|_s^2 \right) (V^2 - 2 \ln V - 1) - 2N_s \left[V + \frac{1}{V} - 2 \right] \left(\left| \frac{A_s}{2} \right|^2 - (V^2 - 2 \ln V - 1) \right) \right]^{1/2}, \quad (18a)$$

$$\frac{\partial N}{\partial \xi} = \frac{N}{V} \frac{\partial V}{\partial \xi}. \quad (18b)$$

The choice of signs in Eq. (18a) depends on the direction of plasma flow.

Given the boundary conditions, the self-consistent profile of V between V_1 and V_2 can be found from Eq. (18a), and the corresponding profiles of N and $|A|^2$ can be obtained from Eqs. (4) and (5). The density scale length of plasma is determined by

$$kL = |N/(\partial N/\partial \xi)| = |V/(\partial V/\partial \xi)|. \quad (18c)$$

III. THREE-PARAMETER FAMILY OF SOLUTIONS

The preceding derivation has established the self-consistent connections between V , N , $|A|^2$, $\partial V/\partial \xi$, $\partial |A|^2/\partial \xi$, N_s , $|A_s|^2$, and $|\partial A/\partial \xi|_s^2$ for a complex field. In order to correctly describe the related physical phenomena, it is necessary to further derive the relation between A_0^2 and $|A_s|^2$. As it is noted, V and N cannot equal zero, otherwise $\ln V$ and $\ln N$ become divergent, and the self-consistent relation cannot be smoothly matched with a rest upstream of plasma ($V=0$) and a plane electromagnetic wave in a vacuum ($N=0$). This means that the velocity is limited between the maximum V_1 and the minimum V_2 . Substituting

$$V = V_2, \quad |A| = |A_2|, \quad \left| \frac{\partial A}{\partial \xi} \right|^2 = \left| \frac{\partial A}{\partial \xi} \right|_2^2 \quad (19)$$

into Eqs. (10), (12), (18a), and (16), we obtain

$$|A_s|^2 - |A_2|^2 = 2(V_2^2 - 2 \ln V_2 - 1), \quad (20)$$

$$N_s = \frac{|A_s|^2 + \left| \frac{\partial A}{\partial \xi} \right|_s^2 - \left| \frac{\partial A}{\partial \xi} \right|_2^2 - |A_2|^2}{4(V_2 + 1/V_2 - 2)}, \quad (21)$$

$$N_2 = \frac{|A_s|^2 + \left| \frac{\partial A}{\partial \xi} \right|_s^2 - \left| \frac{\partial A}{\partial \xi} \right|_2^2 - |A_2|^2}{4(V_2 - 1)^2}, \quad (22)$$

$$\left(\frac{\partial V}{\partial \xi} \right)_2 = \pm \frac{V_2}{|V_2^2 - 1|} \left[\frac{1}{4} |A_2|^2 \left| \frac{\partial A}{\partial \xi} \right|_2^2 - \frac{1}{4} |A_s|^2 \left| \frac{\partial A}{\partial \xi} \right|_s^2 \right]^{1/2}, \quad (23)$$

and

$$Q(V_2) = \frac{(1 - N_2) |A_2|^2 - \left| \frac{\partial A}{\partial \xi} \right|_2^2}{V_2 - 1/V_2}. \quad (24)$$

From Eqs. (23) and (24) and the condition that V_2 is the minimum velocity, namely, $(\partial V/\partial \xi)_2 = 0$ and $(\partial^2 V/\partial \xi^2)_2 \geq 0$, we can obtain

$$|A_2|^2 \left| \frac{\partial A}{\partial \xi} \right|_2^2 = |A_s|^2 \left| \frac{\partial A}{\partial \xi} \right|_s^2 \quad (25)$$

and

$$\frac{1}{(V_2 - 1/V_2)} \left[(1 - N_2) |A_2|^2 - \left| \frac{\partial A}{\partial \xi} \right|_2^2 \right] \geq 0. \quad (26)$$

Using Eqs. (20), (21), and (25), we obtain

$$\left| \frac{\partial A}{\partial \xi} \right|_s^2 = \left[1 - \frac{4N_2 V_2 \left[V_2 + \frac{1}{V_2} - 2 \right]}{2(V_2^2 - 2 \ln V_2 - 1)} \right] |A_s|^2 - 2(V_2^2 - 2 \ln V_2 - 1) + 4N_2 V_2 \left[V_2 + \frac{1}{V_2} - 2 \right]. \quad (27)$$

Substituting $V = V_1$, $|A| = |A_1|$, and $|\partial A/\partial \xi|^2 = |\partial A/\partial \xi|_1^2$ into Eqs. (10), (12), (18a), and (16), we obtain

$$|A_1|^2 = |A_s|^2 + 2(V_1^2 - 2 \ln V_1 - 1), \quad (28)$$

$$\left| \frac{\partial A}{\partial \xi} \right|_1^2 = \left| \frac{\partial A}{\partial \xi} \right|_s^2 + 2(V_1^2 - 2 \ln V_1 - 1) - 4N_1 V_1 \left[V_1 + \frac{1}{V_1} - 2 \right], \quad (29)$$

$$\left(\frac{\partial V}{\partial \xi} \right)_1 = \pm \frac{V_1}{|V_1^2 - 1|} \left[\frac{1}{4} |A_1|^2 \left| \frac{\partial A}{\partial \xi} \right|_1^2 - \frac{1}{4} |A_2|^2 \left| \frac{\partial A}{\partial \xi} \right|_2^2 \right]^{1/2}, \quad (30)$$

and

$$Q(V_1) = \frac{(1-N_1)|A_1|^2 - \left| \frac{\partial A}{\partial \xi} \right|_1^2}{(V_1 - 1/V_1)}. \tag{31}$$

From Eqs. (30) and (31) and the condition that V_1 is the maximum velocity, namely, $(\partial V/\partial \xi)_1 = 0$ and $(\partial^2 V/\partial \xi^2)_1 \leq 0$, we obtain

$$|A_1|^2 \left| \frac{\partial A}{\partial \xi} \right|_1^2 = |A_s|^2 \left| \frac{\partial A}{\partial \xi} \right|_s^2 \tag{32}$$

$$\frac{1}{(V_1 - 1/V_1)} \left[(1-N_1)|A_1|^2 - \left| \frac{\partial A}{\partial \xi} \right|_1^2 \right] \leq 0. \tag{33}$$

Using Eqs. (28), (29), and (30), we get

$$\left| \frac{\partial A}{\partial \xi} \right|_s^2 = \left[1 - \frac{4N_2V_2 \left[V_1 + \frac{1}{V_1} - 2 \right]}{2(V_1^2 - 2 \ln V_1 - 1)} \right] |A_s|^2 - 2(V_1^2 - 2 \ln V_1 - 1) + 4N_2V_2 \left[V_1 + \frac{1}{V_1} - 2 \right]. \tag{34}$$

and

The combination of Eqs. (27) and (34) gives

$$\begin{aligned} |A_s|^2 = & \left\{ 4N_2V_2 \left[\left[V_2 + \frac{1}{V_2} - 2 \right] - \left[V_1 + \frac{1}{V_1} - 2 \right] \right] + 2[(V_1^2 - 2 \ln V_1 - 1) - (V_2^2 - 2 \ln V_2 - 1)] \right\} \\ & \times \left[4N_2V_2 \left[\frac{\left[V_2 + \frac{1}{V_2} - 2 \right]}{2(V_2^2 - 2 \ln V_2 - 1)} - \frac{\left[V_1 + \frac{1}{V_1} - 2 \right]}{2(V_1^2 - 2 \ln V_1 - 1)} \right] \right]^{-1}. \end{aligned} \tag{35}$$

Equation (35) gives the connection among the four quantities N_2 , V_2 , V_1 , and $|A_s|^2$. If three of the quantities are given, the other quantity is determined. However, the quantities obtained in this way are not necessarily reasonable. The requirements that $|A_1|^2 \geq 0$, $|A_2|^2 \geq 0$, $(\partial A/\partial \xi)_1^2 \geq 0$, $(\partial A/\partial \xi)_2^2 \geq 0$, $(1-N_s)|A_s|^2 \geq (\partial A/\partial \xi)_s^2$, $(1-N_1)|A_1|^2 \leq (\partial A/\partial \xi)_1^2$, and $(1-N_2)|A_2|^2 \leq (\partial A/\partial \xi)_2^2$ give the following additional limitations:

$$|A_s|^2 \geq 2(V_1^2 - 2 \ln V_1 - 1), \tag{36}$$

$$|A_s|^2 \geq 2(V_2^2 - 2 \ln V_2 - 1), \tag{37}$$

$$\left[1 - \frac{4N_2V_2 \left[V_1 + \frac{1}{V_1} - 2 \right]}{2(V_1^2 - 2 \ln V_1 - 1)} \right] |A_s|^2 \geq 0, \tag{38}$$

$$\left[1 - \frac{4N_2V_2 \left[V_2 + \frac{1}{V_2} - 2 \right]}{2(V_2^2 - 2 \ln V_2 - 1)} \right] |A_s|^2 \geq 0, \tag{39}$$

$$\left[N_2V_2 - \frac{4N_2V_2 \left[V_2 + \frac{1}{V_2} - 2 \right]}{2(V_2^2 - 2 \ln V_2 - 1)} \right] |A_s|^2 \leq 2(V_2^2 - 2 \ln V_2 - 1) - 4N_2V_2 \left[V_2 + \frac{1}{V_2} - 2 \right], \tag{40}$$

$$\left[\frac{4N_2V_2 \left[V_1 + \frac{1}{V_1} - 2 \right]}{2(V_1^2 - 2 \ln V_1 - 1)} - N_2V_2 \right] |A_s|^2 \leq 2(V_1^2 - 2 \ln V_1 - 1) \left[1 - \frac{N_2V_2}{V_1} \right], \tag{41}$$

$$2(N_2 - 1)(V_2^2 - 2 \ln V_2 - 1) \leq \left[N_2 - \frac{4N_2V_2 \left[V_2 + \frac{1}{V_2} - 2 \right]}{2(V_2^2 - 2 \ln V_2 - 1)} \right] |A_s|^2. \tag{42}$$

Choosing three quantities satisfying conditions (36)–(42), we can find the fourth quantity from Eq. (35) and obtain other quantities from Eqs. (34), (28), (20), (29), (21), and (4). It means that a self-consistent steady-state structure between V_1 and V_2 is determined by three parameters. For example, if $N_1=0.04$, $V_1=2.5$, and $V_2=0.15$, and if $(1-N_2)|A_2|^2 < |(\partial A/\partial \xi)|_2^2$ is satisfied, then we obtain $N_2=0.6667$, $N_2=0.1$, $|A_s|^2=9.5672$, $|A_1|^2=6.1498$, $|A_2|^2=3.93372$, $|(\partial A/\partial \xi)|_1^2=6.8348$, $|(\partial A/\partial \xi)|_2^2=6.6594$, and $|(\partial A/\partial \xi)|_s^2=2.9524$. Such a structure has the velocity and density profiles which spatially oscillate with equal amplitude and equal wavelength. If $(1-N_2)|A_2|^2 = |(\partial A/\partial \xi)|_2^2$, the calculation yields $N_2 > 1$, $|A_2|^2=0$, and $|(\partial A/\partial \xi)|_2^2=0$. This is practically a one-parameter family of solutions. If $(1-N_s)|A_s|^2 = |(\partial A/\partial \xi)|_s^2$, we obtain $V_1=V_2=1$, $|A_1|^2 = |A_2|^2 = |A_s|^2$, $N_1=N_2=N_s$, and

$$\begin{aligned} |(\partial A/\partial \xi)|_1^2 &= |(\partial A/\partial \xi)|_2^2 = |(\partial A/\partial \xi)|_s^2 \\ &= (1-N_s)|A_s|^2. \end{aligned}$$

This is a two-parameter family of solutions. Therefore the obtained self-consistent relations are more general.

IV. BOUNDARY AND JUNCTION CONDITIONS

Our discussion here is confined to the plateau structure which corresponds to

$$|A_s|^2 = 2(V_2^2 - 2 \ln V_2 - 1) = 2(V_1^2 - 2 \ln V_1 - 1), \quad (43)$$

$$\left| \frac{\partial A}{\partial \xi} \right|_s = \left| \frac{\partial A}{\partial \xi} \right|_2 = 0, \quad (44)$$

$$|A_1|^2 = |A_2|^2 = 0, \quad (45)$$

$$\left| \frac{\partial A}{\partial \xi} \right|_1^2 = 2(V_1^2 - 2 \ln V_1 - 1) - 4N_2 V_2 \left[V_1 + \frac{1}{V_1} - 2 \right], \quad (46)$$

$$N_2 = \frac{2(V_2^2 - 2 \ln V_2 - 1)}{4(V_2 - 1)^2}, \quad (47)$$

and

$$N_s = N_2 V_2 = N_1 V_1. \quad (48)$$

The practical boundary conditions are

$$A = A_{0i} e^{i\xi} + A_{0r} e^{-i\xi}, \quad N = 0 \quad \text{as } \xi \rightarrow \infty \quad (49)$$

and

$$|A| = \left| \frac{\partial A}{\partial \xi} \right| = 0, \quad N = N_r, \quad V = 0 \quad \text{as } \xi \rightarrow -\infty, \quad (50)$$

where A_{0i} and A_{0r} are the incident and reflected light intensities, N_r is the plasma density at rest upstream. Obviously, the steady-state plateau structure cannot be naturally joined to such a boundary. This is because the laser-plasma interaction occurs in limited time, and it

takes unlimited time to reach an exact steady state. A reasonable treatment scenario is that the upper and lower density shelves are joined to an isothermal rarefaction wave, respectively.

In the region where the ponderomotive force vanishes, the density is independent of the field A and the plasma expands self-similarly. Solving Eqs. (1)–(2) in the absence of an electromagnetic wave, we readily obtain the self-similar solution

$$V_0 = 1 + \xi/kL_t, \quad (51)$$

$$N_0 = N_r \exp(-1 - \xi/kL_t), \quad (52)$$

where $L_t = C_s t \cos \theta$. Because N is related to t , besides having the high-frequency dependence, the amplitude $E(x, t)$ of the field $E = E(x, t) e^{i\omega t}$ will slowly vary with t . Therefore Eq. (3) can be written as

$$\begin{aligned} \frac{\partial^2 E(x, t)}{\partial x^2} + \frac{\omega^2}{c^2} \epsilon E(x, t) \\ - 2i \frac{\omega}{c} \frac{\partial \epsilon}{\partial t} E(x, t) - \frac{2}{c^2} \frac{\partial \epsilon}{\partial t} \frac{\partial E(x, t)}{\partial t} \\ - \frac{1}{c^2} \frac{\partial^2 \epsilon}{\partial t^2} E(x, t) - \frac{\epsilon}{c^2} \frac{\partial^2 E(x, t)}{\partial t^2} = 0. \end{aligned}$$

Since $|\partial \epsilon / \epsilon \partial t| \ll \omega$, $|\partial E / E \partial t| \ll \omega$, $|\partial^2 \epsilon / \epsilon \partial t^2| \ll \omega^2$, and $|\partial^2 E / E \partial t^2| \ll \omega^2$, as a reasonable approximation, the terms associated with them are omitted. Equation (6) still holds for the region where $d|A|^2/d\xi = 0$ and $N = N_0 = N_r \exp(-1 - \xi/kL_t)$. Then the time t may be regarded as a parameter. Inserting Eq. (52) into Eq. (6), we can find the electric field corresponding to the density N_0 at any time t ,

$$A_0 = C_1 H_\nu^{(1)}(\nu N_0^{1/2}) + C_2 H_\nu^{(2)}(\nu N_0^{1/2}), \quad (53)$$

where $H_\nu^{(1)}(\nu N_0^{1/2})$ and $H_\nu^{(2)}(\nu N_0^{1/2})$ are the Hankel functions of order ν , and $\nu = i2kL_t$. We use the uniform asymptotic expansions for the Hankel functions with $|\nu| \gg 1$ and only retain the dominant terms. The expression for the electric field (53) reduces to

$$\begin{aligned} A_0 = \frac{(4\xi/1 - N_0)^{1/4}}{(2kL_t)^{1/3}} \{ [(2b - d) + i(c - 2a)] \text{Ai}(-z) \\ + (c + id) \text{Bi}(-z) \}, \quad (54) \end{aligned}$$

with

$$\begin{aligned} \frac{2}{3} \xi^{3/2} = \ln[1 + (1 - N_0)^{1/2} - \frac{1}{2} \ln N_0 - (1 - N_0)^{1/2}] \\ (N_0 < 1), \end{aligned}$$

$$\frac{2}{3} (-\xi)^{3/2} = (N_0 - 1)^{1/2} - \arccos(1/N_0^{1/2}) \quad (N_0 > 1).$$

Here $C_1 = a + ib$, $C_2 = c + id$, $z = (2kL_t)^{2/3} \xi$, and a , b , c , and d are four real constants to be determined. $\text{Ai}(-z)$ and $\text{Bi}(-z)$ are Airy functions. In the underdense region, using the asymptotic expansions of Airy functions for $kL_t \gg 1$, we obtain

$$|A_0|^2 = \frac{(c^2+d^2)}{\pi k L_t (1-N_0)^{1/2}} + \frac{1}{\pi k L_t (1-N_0)^{1/2}} [4(a^2+b^2)-4(ac+bd)] \sin^2 \left[\frac{4}{3} k L_t \xi^{3/2} + \frac{\pi}{4} \right] + \frac{2}{\pi k L_t (1-N_0)^{1/2}} (bc-ad) \sin \left[\frac{8}{3} k L_t \xi^{3/2} + \frac{\pi}{2} \right], \tag{55}$$

$$\left| \frac{\partial A_0}{\partial \xi} \right|^2 = \frac{(1-N_0)^{1/2}}{\pi k L_t} \left[[4(a^2+b^2)-4(ac+bd)] \cos^2 \left[\frac{4}{3} k L_t \xi^{3/2} + \frac{\pi}{4} \right] + (c^2+d^2) - 2(bc-ad) \sin \left[\frac{8}{3} k L_t \xi^{3/2} + \frac{\pi}{2} \right] \right], \tag{56}$$

and

$$\frac{d|A_0|^2}{d\xi} = (-16|C_1|^2 + 8C_1^*C_2 + 8C_1C_2^* - 4|C_2|^2) \text{Ai}(-z)\text{Ai}'(-z) - 4|C_2|^2 \text{Bi}(-z)\text{Bi}'(-z) - i4(C_1^*C_2 - C_1C_2^*) [\text{Ai}'(-z)\text{Bi}(-z) + \text{Ai}(-z)\text{Bi}'(-z)], \tag{57}$$

where

$$\begin{aligned} \text{Ai}(-z)\text{Ai}'(-z) &= -\text{Bi}(-z)\text{Bi}'(-z) \\ &= -\frac{1}{2}\pi^{-1} \sin \left[\frac{8}{3} k L_t \xi^{3/2} + \frac{\pi}{2} \right], \end{aligned}$$

$$\begin{aligned} \text{Ai}'(-z)\text{Bi}(-z) + \text{Ai}(-z)\text{Bi}'(-z) &= -\pi^{-1} \cos \left[\frac{8}{3} k L_t \xi^{3/2} + \frac{\pi}{2} \right]. \end{aligned}$$

In order to guarantee the validity of the self-similar solution in the range $\xi_{lt} \leq \xi < \infty$, we demand that

$$\frac{d|A_0|^2}{d\xi} = 0 \text{ for } \xi_{lt} \leq \xi < \infty.$$

Then we have

$$8C_1^*C_2 + 8C_1C_2^* = 16|C_1|^2$$

and

$$C_1^*C_2 = C_1C_2^*,$$

i.e.,

$$ac + bd = a^2 + b^2, \tag{58}$$

$$bc = ad. \tag{59}$$

As $\xi \rightarrow \infty$, Eq. (54) gives

$$\begin{aligned} A_0 &= \frac{1}{(\pi k L_t)^{1/2} (1-N_0)^{1/4}} \left[(c-a) \cos \left[2k L_t (\ln 2 - 1) + \frac{\pi}{4} \right] + (b-d) \sin \left[2k L_t (\ln 2 - 1) + \frac{\pi}{4} \right] \right. \\ &\quad \left. + i(c-a) \sin \left[2k L_t (\ln 2 - 1) + \frac{\pi}{4} \right] - i(b-d) \cos \left[2k L_t (\ln 2 - 1) + \frac{\pi}{4} \right] \right] e^{i\xi} \\ &\quad + \frac{1}{(\pi k L_t)^{1/2} (1-N_0)^{1/4}} \left[a \cos \left[2k L_t (\ln 2 - 1) + \frac{\pi}{4} \right] + b \sin \left[2k L_t (\ln 2 - 1) + \frac{\pi}{4} \right] \right. \\ &\quad \left. + ib \cos \left[2k L_t (\ln 2 - 1) + \frac{\pi}{4} \right] - ia \sin \left[2k L_t (\ln 2 - 1) + \frac{\pi}{4} \right] \right] e^{-i\xi}. \end{aligned} \tag{60}$$

The vacuum boundary condition (49) and Eqs. (58) and (59) give

$$\begin{aligned} |A_{0i}|^2 &= \frac{1}{\pi k L_t} [(c^2+d^2) - (a^2+b^2)] \\ &= \frac{(c^2+d^2)}{\pi k L_t} - |A_{0r}|^2, \end{aligned} \tag{61}$$

$$|A_{0r}|^2 = \frac{(a^2+b^2)}{\pi k L_t}. \tag{62}$$

Substituting Eqs. (59), (61), and (62) into Eqs. (55) and (56), we obtain, in the range $\xi_{lt} \leq \xi < \infty$,

$$|A_0|^2 = \frac{(c^2 + d^2)}{\pi k L_t (1 - N_0)^{1/2}} = \frac{(1 + \beta) |A_{0i}|^2}{(1 - N_0)^{1/2}}, \quad (63)$$

$$\left| \frac{\partial A_0}{\partial \xi} \right|^2 = (1 - N_0)^{1/2} (1 + \beta) |A_{0i}|^2, \quad (64)$$

where $\beta \equiv |A_{0r}|^2 / |A_{0i}|^2$ is the reflection coefficient.

Now we consider the junction conditions. Let ξ_{lt} be the joint point of the rarefaction wave with the lower density shelf. Then in the range $\xi_{lt} \leq \xi < \infty$ we have

$$\left| \frac{\partial N_0}{\partial \xi} \right| = \left| -\frac{\partial V_0}{\partial \xi} \right| = \left| -\frac{1}{k L_t} \right|, \quad (65)$$

$$\frac{d |A_0|^2}{d \xi} = 0, \quad (66)$$

and for $-\infty < \xi \leq \xi_{lt}$,

$$\left| \frac{\partial N}{\partial \xi} \right| = \left| -\frac{\partial V}{\partial \xi} \right| = \left| \frac{|A|}{2 |V^2 - 1|} \frac{\partial A}{\partial \xi} \right| \quad (V \neq 1), \quad (67)$$

$$\left| \frac{\partial N}{\partial \xi} \right| = \left| \frac{\partial V}{\partial \xi} \right| = \frac{1}{2} (1 - N_s)^{1/2} |A_s| \quad (V = 1). \quad (68)$$

The equalities

$$N_{0r} = N_t, \quad (69)$$

$$V_{0r} = V_t, \quad (70)$$

$$\left[\frac{\partial N_0}{\partial \xi} \right]_t = \left[\frac{\partial N}{\partial \xi} \right]_t, \quad (71)$$

$$\left[\frac{\partial V_0}{\partial \xi} \right]_t = \left[\frac{\partial V}{\partial \xi} \right]_t, \quad (72)$$

and

$$\frac{d |A_0|^2}{d \xi} = \frac{d |A|^2}{d \xi} = 0 \quad (73)$$

all hold only if

$$\xi_{lt} = 0 \quad (74)$$

and

$$\frac{1}{k L_t} = \frac{1}{2} (1 - N_s)^{1/2} |A_s|. \quad (75)$$

Thus the junction conditions should be

$$N_{0r} = N_s, \quad (76)$$

$$V_{0r} = V_s = 1, \quad (77)$$

$$|A_0|^2 = |A_s|^2, \quad (78)$$

$$\frac{1}{k L_t} = \frac{1}{2} (1 - N_s)^{1/2} |A_s|,$$

where

$$|A_0|^2 = \frac{(1 + \beta) |A_{0i}|^2}{(1 - N_{0r})^{1/2}}, \quad (79)$$

$$|A_s|^2 = 2(V_2^2 - 2 \ln V_2 - 1), \quad (80)$$

$$N_s = N_2 V_2, \quad (81)$$

$$N_2 = |A_s|^2 / 4(V_2 - 1)^2, \quad (82)$$

$$N_{0r} = N_{0i} \exp \left[-1 - \frac{\xi_{lt}}{k L_t} \right] = N_{0i} \exp(-1). \quad (83)$$

There are ten equations (76)–(83) and twelve quantities: N_{0r} , N_s , V_{0r} , V_s , $|A_{(0)}|_t$, $|A_s|$, $k L_t$, β , A_{0i} , V_2 , N_2 , and N_{0i} . Therefore this is a two-parameter family of solutions. Generally speaking, $|A_{0i}|^2$ and β are given as known measurable quantities. The previous results are only the special cases for $\beta = 0$ (Ref. 2) or $\beta = 1$.⁴

In order to match the steady-state structure with the rest upstream, we consider the junction conditions at the upper density shelf. Let ξ_{ht} be the joint point of the rarefaction wave with the upper density shelf. Then the junction conditions should be

$$|A|^2 = \left| \frac{\partial A}{\partial \xi} \right|^2 = \frac{d |A|^2}{d \xi} = 0, \quad (84)$$

$$V_2 = V_{ht} = 1 + \frac{\xi_{ht}}{k L_t}, \quad (85)$$

and

$$N_2 = N_r \exp \left[-1 - \frac{\xi_{ht}}{k L_t} \right]. \quad (86)$$

Equation (85) gives

$$\xi_{ht} = k L_t (V_2 - 1) \quad (87)$$

and Eq. (86) gives

$$N_r = N_2 \exp(V_2). \quad (88)$$

Here $\partial V / \partial \xi$ and $\partial N / \partial \xi$ are not continuous at $\xi = \xi_{ht}$, and ξ_{ht} is a weakly discontinuous point. From the above results, the spatial distributions of N and $|A|^2$ for $-\infty < \xi < \infty$ can completely be determined.

V. COMPARISON WITH PREVIOUS RESULTS AND EXPERIMENTS

In order to directly perceive the characteristics of the field structure and density profile in the plasma and judge accuracy of our treatment, we show the preceding results in Figs. 1–3. The ponderomotive-force potential and density profile in the plasma are shown in Fig. 1. The dot-dashed curve indicates the spatial distribution of $|A|^2$ at $A_{0i} = 0.62$ and $\beta = 1$. The dashed curve indicates the self-consistent density profile N under the action of the ponderomotive force. The result is closer to the rarefaction wave plateaus given in Ref. 1: The density profile developed under the action of the ponderomotive

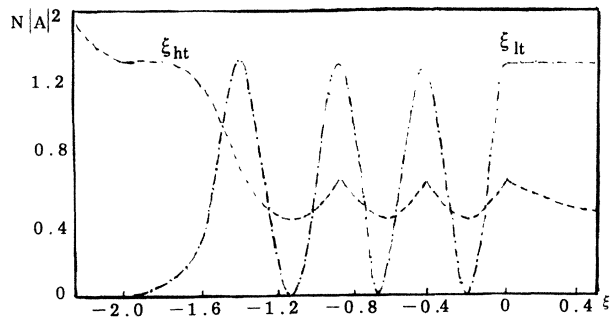


FIG. 1. $|A|^2$ and N vs ξ . Dot-dashed curve, $|A|^2$ versus ξ at $A_{0i}=0.62$ and $\beta=1$; Dashed curve, N versus ξ at $A_{0i}=0.62$ and $\beta=1$ under the action of the ponderomotive force.

force consists of a modulated lower density, a linear distribution with a steep rise near the critical density region, and an upper-density shelf where it is attached to the extra-high-density region by a rarefaction wave. The lower-density shelf is connected with a rarefaction wave at $\xi=\xi_{lt}$. The upper-density shelf is connected with a rarefaction wave at $\xi=\xi_{ht}$. The spatial distribution of N in the region $\xi_{lt} \geq \xi \geq \xi_{ht}$ is obtained by integrating Eq. (18b). The number of extreme points depends on the distance between the upper and lower limits of integration and the value of N_s ($|A_s|^2$). The positive and negative signs in front of Eq. (18a) lead to the appearance of cusps in the lower-density shelf. The spatial distribution of $|A|^2$ is obtained by integrating Eq. (7), and $d|A|^2/d\xi=0$, which is determined by $V=1$, is independent of the signs of $dV/d\xi$. Therefore, in contrast to the density N , the distribution of $|A|^2$ has the extreme values rather than the cusps.

Figure 2 shows the variation of the density step height N_2 with $I_0\lambda^2$. The curve *A* is a plot of experimental result in Ref. 5, and the curves *B*, *C*, and *D* correspond to the results of Lee *et al.*,² Estabrook and Kruer,³ and Xu *et al.*,⁴ respectively. The curve *E* corresponds to our result. As seen, curve *E* lies between curves *B* and *D*, and curve *C* is only in agreement with curve *E* for the lower incident light intensity.

The values N_2 given by the curves *B*, *C*, *D*, and *E* are lower than the experimental value. The diversity of curves *B*, *C*, *D*, and *E* comes from the different connection conditions and treatment methods used. Their deviation from the experiment (curve *A*) is caused by the isothermal model.

Figure 3 shows the dependence of the density scale lengths L_c (curves *A* and *B*) and L_s (curve *C*) on the incident intensity I_0 and the reflection coefficient β . As is seen from curves *A* and *B* in Fig. 3, the value of L_c for $\beta=0$ (curve *B*) is greater than that at the same intensity for $\beta=1$ (curve *A*). If β is different in the discussed density region, then the value of L_c will scatter. If β takes a smaller value in the higher-intensity region, then the value of L_c may increase. We also see that the value of L_c reduces with the rise of I_0 at the different rates in the lower- and higher-intensity regions. The calculation

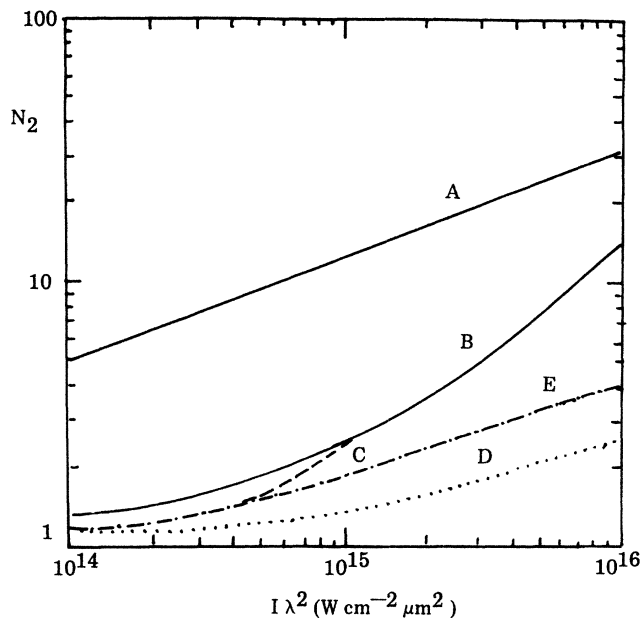


FIG. 2. $I_0\lambda^2$ dependence of density step height N_2 . Curve *A*, the values measured in Ref. 5; curve *B*, the values predicted in Ref. 2 ($T_e=250$ eV); curve *C*, the values predicted in Ref. 3 ($T_e=250$ eV); curve *D*, the values predicted in Ref. 4 ($T_e=250$ eV); curve *E*, the values predicted in our model ($T_e=250$ eV).

shows that $L_c \sim I_0^{-1.4}$ for $I_0 < 10^{13}$ W cm⁻² and $\beta=1$, which is steeper than the scaling law $L_c \sim I_0^{-1}$ predicted by Lee *et al.*, and that $L_c \sim I_0^{-0.25}$ for $I_0 > 10^{13}$ W cm⁻² and $\beta=1$, which is gentler than Lee *et al.*'s. In particular, we find that the value of L_c at $I_0=10^{13}$ W cm⁻² and $\beta=1$ is 3 μ m. The above results are in good agreement with the experiment.⁵ As we see from the curves *A* and *C* ($\beta=1$) in Fig. 3, $L_s < L_c$ for lower I_0 , $L_c < L_s$ for higher I_0 , and both are close to each other for higher I_0 .

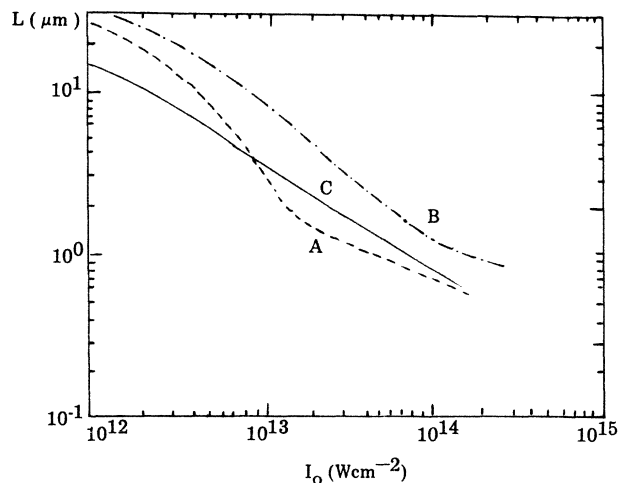


FIG. 3. Variations of density scale lengths with I_0 at $T_e=250$ eV and $\lambda=10.6$ μ m. Curve *A*, the variation of L_c with I_0 ($\beta=1$); curve *B*, the variation of L_c with I_0 ($\beta=0$); curve *C*, the variation of L_s with I_c ($\beta=1$).

VI. SUMMARY

We have derived the self-consistent relations between V , N , $|A|^2$, $|A_s|^2$, and $\partial V/\partial \xi$ for a complex field. The relation between $|A_{0i}|$ and $|A_s|$ has also been established in our steady-state model. Although the expression for $\partial V/\partial \xi$ in the steady-state model is formally identical with Xu *et al.*'s for the plateau structure, the boundary condition in a vacuum and the junction condition of $\partial N/\partial \xi$ at the joint point cannot be satisfied in

their treatment limited to a real field. For a complex field the required boundary and junction conditions should be the continuity of A , A^* , $\partial A/\partial \xi$, and $\partial A^*/\partial \xi$ rather than $|A|$ and $|\partial A/\partial \xi|$ at the boundary and joint points. For lack of the information on $(\partial A/\partial \xi)_i$ in the self-consistent treatment, we find the relation between $|A_{0i}|^2$ and $|A_s|^2$ from the requirement of the continuity of $d|A|^2/d\xi$, $\partial V/\partial \xi$, and $\partial N/\partial \xi$. Our treatment is completely self-consistent because $d|A|^2/d\xi=0$ for $\infty > \xi_{it} \geq 0$.

- ¹R. D. Jones, C. H. Aldrich, and K. Lee, *Phys. Fluids* **24**, 310 (1981).
²K. Lee, D. W. Forslund, J. M. Kindel, and E. L. Lindman, *Phys. Fluids* **20**, 51 (1977).
³K. Estabrook and W. L. Krueer, *Phys. Fluids* **26**, 1888 (1983).
⁴Zhi-Zhan Xu, Wei Yu, and Wen-Qi Chang, *Phys. Rev. A* **32**, 659 (1985).
⁵R. Fedosejevs, M. D. J. Burgess, G. D. Enright, and M. C. Richardson, *Phys. Fluids* **24**, 537 (1981).
⁶C. E. Max, in *Laser-Plasma Interaction*, edited by Roger Belian and Jean-Claude Adam (North-Holland, New York, 1982), p. 304.
⁷*Handbook of Mathematical Functions with Formulas, Graphs,*

- and Mathematical Tables*, Natl. Bur. Stand. Appl. Math. Ser. No. 55, edited by M. Abramowitz and I. A. Stegun (U.S. GPO, Washington, D.C., 1964), p. 368.
⁸P. Mulser and C. Van Kessel, *Phys. Rev. Lett.* **38**, 902 (1977).
⁹D. W. Forslund, J. M. Kindel, K. Lee, and E. L. Lindman, *Phys. Rev. Lett.* **36**, 35 (1976).
¹⁰R. L. Stenzel, A. Y. Wong, and H. C. Kim, *Phys. Rev. Lett.* **52**, 654 (1973); H. C. Kim, R. Stenzel, and A. Y. Wong, *ibid.* **33**, 886 (1974).
¹¹R. Hofstauter, *Laser Res.* **8**, 180 (1980); E. Fabre, *ibid.* **8**, 28 (1980).
¹²O. Willi, R. G. Evans, and A. Raven, *Phys. Fluids* **23**, 2061 (1980).